

Radiative cooling of nanoparticles close to a surface

M. Tschikin and S.-A. Biehs

Institut für Physik, Carl von Ossietzky Universität, D-26111 Oldenburg, Germany.

F.S.S. Rosa and P. Ben-Abdallah

*Laboratoire Charles Fabry, UMR 8501, Institut d'Optique, CNRS,
Université Paris-Sud 11, 2, Avenue Augustin Fresnel, 91127 Palaiseau Cedex, France.*

(Dated: October 14, 2018)

We study the radiative cooling of polar and metallic nanoparticles immersed in a thermal bath close to a partially reflecting surface. The dynamics of relaxation is investigated at different distances from the surface, i.e., in the near-field and far-field zones. We demonstrate the existence of an oscillating behavior for the thermal relaxation time with respect to the separation distance from the surface, an analog of Friedel oscillations in Fermi liquids.

PACS numbers: 44.40.+a, 78.20.-e, 78.67.-n, 03.50.De

I. INTRODUCTION

It is well known since the pioneering works of Drexhage *et al.* [1] and Chance *et al.* [2] on the molecular fluorescence emission that the radiative lifetime of excited atoms or molecules is not an intrinsic property of matter, but it depends on their close environment [3, 4]. This de-excitation process is accompanied by spontaneous light emission, that can be investigated by either a classical or quantum approach. From a classical point of view, the atom/molecule is considered as a simple dipole that radiates as an antenna. The radiated field is then found with the help of Maxwell's equations and the spontaneous decay rate is proportional to the partial local density of states [5, 6]. On the other hand, from a quantum point of view, the process is described as a transition between different discrete states of the atom/molecule. The radiative lifetime or its emission rate is then straightforwardly deduced by application of Fermi's golden rule [3, 4, 7].

The radiative cooling of a nano-object is, in a way, a continuous version of the latter. When such an object is thermally excited at a given temperature, a continuum of modes centered around the hot body's thermal frequency is excited according to the Bose-Einstein distribution function. As a result, these modes de-excite throughout heat exchanges with the surrounding environment. As the local temperature decreases during the thermal relaxation process new modes are excited (at smaller frequencies), changing the cooling spectrum as the system is driven towards thermal equilibrium. Understanding the underlying mechanisms for such a non-steady dissipative process is of major importance for controlling the heat flow in nanoscale systems and might be of practical relevance in potential applications such as near-field thermo-photovoltaics [8] and thermal management in microelectronics [9].

In this work, we describe the dynamic process of thermal relaxation for polar and metallic nanoparticles facing a substrate at a given distance. For the polar material we choose SiC because it supports surface phonon polaritons in the near-infrared. This is due to a negative real part

of the permittivity for frequencies ω in the *reststrahlen* region, i.e. for $\omega_{\text{TO}} < \omega < \omega_{\text{LO}}$, where ω_{TO} and ω_{LO} are the frequencies of the transversal and longitudinal optical phonon, respectively. As we will discuss below the main channel for thermal relaxation will be due to these surface modes. For the metal case we choose Au which can be described by a simple Drude model in the infrared region. In particular, metals like Au have a negative real part of the permittivity for all frequencies ω smaller than the plasma frequency ω_p which is typically one or two orders of magnitudes larger than ω_{TO} . In particular, for Au the surface plasmon polariton resonance lies in the ultraviolet region so that in this case the surface modes play a minor role for thermal relaxation. In fact, for metals the main channel for thermal relaxation is due to the induction of eddy currents.

We compare the dynamic process for both materials considering only particles smaller than the thermal wavelength $\lambda_{\text{th}} = \hbar c / (k_B T)$, where c is the vacuum velocity of light, $2\pi\hbar$ is Planck's constant, k_B is Boltzmann's constant, and T is the particle's temperature. Then we can use the dipole model based on Rytov's fluctuational electrodynamics [10] in order to describe the heat loss of the particle due to radiation. This model has for example been used to determine the heat flux between a spherical nanoparticle and a flat surface [11–16], between a spherical particle and a structured or rough surface [17–20], between ellipsoidal particles and a flat or structured surfaces [21, 22] as well as between two or more spherical particles [23–26] or particles of arbitrary shape [27, 28]. By using the dipole-model, we can introduce the thermal lifetime of a heated particle above a surface analogous to the lifetime of an excited atom or molecule above a surface. We investigate in particular the asymptotic behavior of cooling rates both in near- and far-field regimes and show how the cooling depends on material properties of the particle and the substrate.

The paper is organized as follows: In section II we introduce the dipole model for the heat flux between a particle and a flat surface. In section III we define the thermal relaxation time for small temperature gradients

and discuss it for different distance regimes for polar and metallic nanoparticles. Finally, in section IV we define a general thermal relaxation time and solve the dynamical problem of thermal relaxation of a nanoparticle above a flat surface, numerically.

II. HEAT FLUX BETWEEN A PARTICLE AND A FLAT SURFACE

Let us consider the situation depicted in Fig. 1. A spherical nanoparticle with a radius R is placed in front of a substrate at a fixed distance d . Assuming isotropic, homogeneous and non-magnetic materials, the nanoparticle and the substrate can be characterized by the permittivities ϵ_P and ϵ_S . Furthermore, we assume that the particle's temperature T_P is higher than the temperature of its surroundings T_S . Then the heat flux from the nanoparticle to the substrate due to the imposed temperature gradient can be described within a dipole model [11–14] if the particle radius is much smaller than the thermal wavelength $\lambda_{th,P}$. Including the magnetic response due to the induction of eddy currents in the object, which is important for metals in the infrared region [15, 16, 23, 29], the net power dissipated by the dipole reads [13]

$$\mathcal{P}_{S \leftrightarrow P} = \sum_{i=E,H} \int_0^\infty d\omega \, 2\omega \, \text{Im}(\alpha^i) D^i(\omega, d) \Delta\Theta(\omega, T_P, T_S), \quad (1)$$

where

$$D^i(\omega, d) = \frac{\omega}{\pi c^2} \text{Im} \, \text{Tr} \, \mathbf{G}^i(\omega; d, d) \quad (2)$$

is the electric ($i=E$) and magnetic ($i=H$) local density of states (LDOS) at a distance d from the surface [30, 31], and $\mathbf{G}^i(\omega; z, z')$ is the dyadic Green tensor of the system (see Appendix A). We also have

$$\begin{aligned} \Delta\Theta(\omega, T_P, T_S) &= \Theta(\omega, T_P) - \Theta(\omega, T_S) \\ &= \frac{\hbar\omega}{e^{\hbar\omega/k_b T_P} - 1} - \frac{\hbar\omega}{e^{\hbar\omega/k_b T_S} - 1}, \end{aligned} \quad (3)$$

which is the difference of the mean energy of harmonic oscillators at temperatures T_P and T_S , respectively. $\text{Im}(\alpha^E)$ and $\text{Im}(\alpha^H)$ are the imaginary parts of the electric and magnetic polarizability of the nanoparticle and will be specified in Eqs. (8)) and (9). The physical interpretation of expression (1) is the following one: The power radiated by a nanoemitter radiates into its environment is a function of the LDOS of the electromagnetic field at the emitter position, which defines all possible channels for radiative and non-radiative exchanges with the background. Note that the above expression does not take into account the interaction with the image dipole [14]. This is reasonable for distances $d^3 \gg R^3 |\epsilon_S - 1| |\epsilon_P - 1| / (4|\epsilon_P + 2| |\epsilon_S + 1|)$ - a condition that is automatically fulfilled when $d \gg R$, where the dipole model is valid.

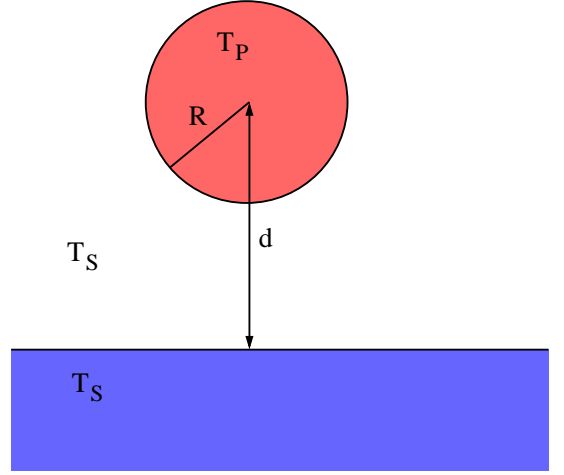


Figure 1: Sketch of a nanoparticle with radius R above a flat surface at a fixed distance d . The nanoparticle has the temperature T_P which is assumed to be larger than the temperature of the surrounding T_S .

Substituting the known Green's functions for a half-space geometry [32, 33] into the definition of the LDOS in Eq. (2) yields [30]

$$\begin{aligned} D^E &= \frac{\omega^2}{2\pi c^3} \int \frac{d^2\kappa}{(2\pi)^2} \frac{e^{-2\text{Im}(\gamma_0)d}}{|\gamma_0|^2} \left[\frac{\text{Re}(\gamma_0)}{k_0} \left(2 + \text{Re}(r_s e^{2i\gamma_0 d}) \right) \right. \\ &\quad + \frac{2\kappa^2 - k_0^2}{k_0^2} \text{Re}(r_p e^{2i\gamma_0 d}) \left. \right] + \frac{\text{Im}(\gamma_0)}{k_0} \left(\text{Im}(r_s) \right. \\ &\quad + \left. \left. \frac{2\kappa^2 - k_0^2}{k_0^2} \text{Im}(r_p) \right) \right] \end{aligned} \quad (4)$$

$$\begin{aligned} D^H &= \frac{\omega^2}{2\pi c^3} \int \frac{d^2\kappa}{(2\pi)^2} \frac{e^{-2\text{Im}(\gamma_0)d}}{|\gamma_0|^2} \left[\frac{\text{Re}(\gamma_0)}{k_0} \left(2 + \text{Re}(r_p e^{2i\gamma_0 d}) \right) \right. \\ &\quad + \frac{2\kappa^2 - k_0^2}{k_0^2} \text{Re}(r_s e^{2i\gamma_0 d}) \left. \right] + \frac{\text{Im}(\gamma_0)}{k_0} \left(\text{Im}(r_p) \right. \\ &\quad + \left. \left. \frac{2\kappa^2 - k_0^2}{k_0^2} \text{Im}(r_s) \right) \right] \end{aligned} \quad (5)$$

where we have introduced the usual Fresnel coefficients for s- and p-polarized waves [34]

$$r_s = \frac{\gamma_0 - \gamma_S}{\gamma_0 + \gamma_S}, \quad (6)$$

$$r_p = \frac{\gamma_0 \epsilon_S - \gamma_S}{\gamma_0 \epsilon_S + \gamma_S} \quad (7)$$

with the z-component of the wave vector in vacuum $\gamma_0 = \sqrt{k_0^2 - \kappa^2}$, the z-component of the wave vector inside the substrate $\gamma_S = \sqrt{k_0^2 \epsilon_S - \kappa^2}$, and the wave number in vacuum $k_0 = \omega/c$. Note, that the electric LDOS can be retrieved from the magnetic LDOS by interchanging $r_s \leftrightarrow r_p$ and vice versa. Furthermore, the electric and magnetic LDOS contain the contribution of propagating modes for lateral wave vectors $\kappa < k_0$ for which $\text{Im}(\gamma_0) = 0$ and the contribution of evanescent modes for which

$\kappa > k_0$ and therefore $\text{Re}(\gamma_0) = 0$. Due to the rotational invariance with respect to rotations around the z -axis, we can reduce (4) and (5) to one dimensional integrals by introducing cylindrical coordinates.

Finally, we need the polarizabilities of the nanoparticle to evaluate expression (1). In the case of a spherical particle of radius R the polarizabilities can be derived from Mie scattering theory [35]. Denoting the particle's relative permittivity by ϵ_P and introducing the dimensionless variables $x = k_0 R$ and $y = \sqrt{\epsilon_P} k_0 R$, one finds [23, 35]

$$\alpha_P^E = 2\pi R^3 \frac{(2\epsilon_P + 1) [\sin(y) - y \cos(y)] - y^2 \sin(y)}{(\epsilon_P - 1) [\sin(y) - y \cos(y)] + y^2 \sin(y)} \quad (8)$$

$$\alpha_P^H = \frac{\pi R^3}{3} \left(\frac{(x^2 - 6)}{y^2} [y^2 + 3y \cot(y) - 3] - \frac{2x^2}{5} \right) \quad (9)$$

for $x \ll 1$, implying that the particle's radius should be small compared to the dominant thermal wavelength, $R \ll \lambda_{th}$. If we demand further that $|y| \ll 1$, i.e. that the radius should be smaller than the skin depth at thermal frequencies, the above expressions reduce to

$$\alpha_P^E = 4\pi R^3 \frac{\epsilon_P - 1}{\epsilon_P + 2}, \quad (10)$$

$$\alpha_P^H = \frac{2\pi}{15} R^3 (k_0 R)^2 (\epsilon_P - 1). \quad (11)$$

We have checked that with the previous expressions we retrieve the dipole contribution to the heat flux for an isolated nanoparticle, i.e., $r_P = r_S = 0$, derived by means of Rytov's fluctuational electrodynamics [36]. Note that in the whole model we have for convenience neglected any nonlocal effects both in the substrate [5, 37–40] and the particle [41, 42].

III. THERMAL RELAXATION TIME OF A SMALL PARTICLE

In the absence of phase transitions, the time evolution of the temperature field of a nanoparticle of heat capacity C_P , mass density ρ and of volume $V = 4\pi R^3/3$ is given by

$$\rho C_P V \frac{dT_P}{dt} = -\mathcal{P}_{S \leftrightarrow P}(T_P). \quad (12)$$

which is just a heat-balance equation. It is important to point out that the substitution of (1) in the r.h.s of (12) is apparently inconsistent, as we are using an expression obtained from the fluctuation dissipation theorem - and therefore assuming local thermal equilibrium - to calculate the cooling rate of a given object, which is clearly a process out-of-equilibrium (even locally). Further investigation, however, shows that here this does not cause any trouble: the characteristic time τ_{ph} for temperature homogenization throughout the body ($\tau_{ph} \lesssim 10^{-8}s$) is, as we shall see, much smaller than the thermal relaxation time (to be defined below). That essentially means

that the particle cools down in a quasi-stationary fashion, which in turn justifies the use of (1) into (12).

Considering a slightly heated nanoparticle with a temperature $T_P = T_S + \Delta T$, a thermal relaxation time τ_ℓ (i.e., the inverse of cooling rate) can be defined by linearization of (12) with respect to the temperature difference ΔT . The resulting linearized equation

$$\frac{dT_P}{dt} = -\frac{1}{\tau_\ell} \Delta T \quad (13)$$

together with (1) leads to

$$\tau_\ell^{-1} = \frac{1}{\rho C_P V} \sum_{i=E,H} \int_0^\infty d\omega \, 2\omega \text{Im}(\alpha^i) D^i(\omega, z) \left. \frac{d\Theta(\omega, T)}{dT} \right|_{T_S}. \quad (14)$$

In Fig. 2 we show the evolution of the thermal relaxation time (TRT) with respect to the separation distance d from the surface for different materials obtained using Eq. (14) together with Eqs. (4)-(9). We first note the presence of two distinct regions for the TRT. When the separation distance is much smaller than the thermal wavelength $\lambda_{th,P}$ we see that the cooling process is faster than for an isolated particle and it decreases drastically as the separation distance is reduced. On the other hand, in the intermediate regime for distances $d \approx \lambda_{th,P}$ we see that the TRT oscillates with respect to d and approaches for large d the (linearized) value $\tau_{0,\ell}$ of an isolated particle, given by [35, 36]

$$\tau_{0,\ell}^{-1} = \frac{1}{\rho C_P V} \sum_{i=E,H} \int_0^\infty d\omega \left(\frac{\omega^3}{\pi^2 c^3} \right) \text{Im}(\alpha^i) \left. \frac{d\Theta(\omega, T)}{dT} \right|_{T_S}. \quad (15)$$

This behavior of the cooling rate demonstrates that we can either reduce or increase the power exchange with the surface for $d \approx \lambda_{th,P}$. In order to get more physical insight, we calculate below the asymptotic behavior of the power exchanged between the substrate and the nanoparticle in these two regimes.

A. Cooling in the near-field regime

The asymptotic expressions for the LDOS in the quasi-static regime, i.e., for distances $z \ll \lambda_{th,P}$ can be derived by considering only contributions for wave vectors $\kappa \gg k_0$. Then one gets the known expressions [30]

$$D^E(\omega, d) \approx \frac{\omega^2}{\pi^2 c^3} \frac{\text{Im}(\epsilon_S)}{|\epsilon_S + 1|^2} \frac{1}{4(k_0 d)^3}, \quad (16)$$

$$D^H(\omega, d) \approx \frac{\omega^2}{\pi^2 c^3} \left[\frac{\text{Im}(\epsilon_S)}{4} + \frac{\text{Im}(\epsilon_S)}{|\epsilon_S + 1|^2} \right] \frac{1}{4(k_0 d)}. \quad (17)$$

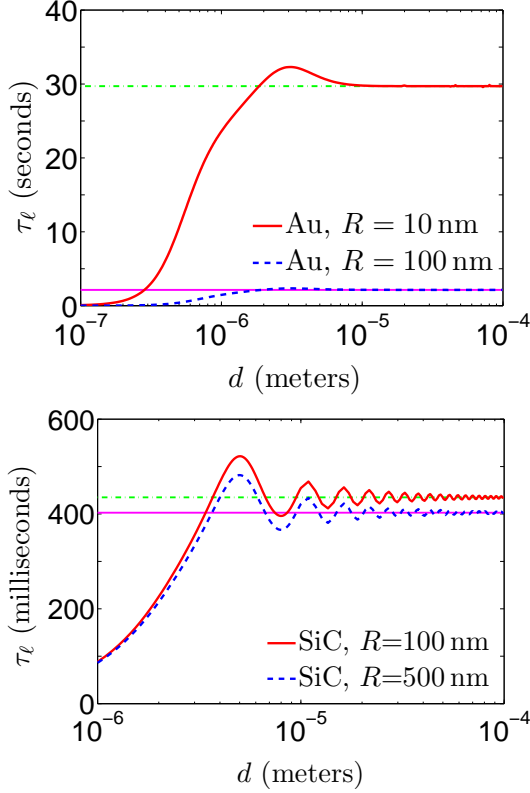


Figure 2: Semi-logarithmic plot of the distance dependence of the TRT of a nanoparticle above a substrate with temperature $T_S = 300$ K (a) for a gold nanoparticle above a gold surface, (b) a SiC nanoparticle above a SiC surface. The horizontal lines mark the asymptotic values given by Eq. (15). For ϵ_P/ϵ_S we use for Au the Drude model and for SiC a Drude-Lorentz model [35, 43]. For ρ we use ρ^{Au} and ρ^{SiC} and for the heat capacity we use a simple Debye model (see appendix C) so that we have at $T_P = 300$ K the values $\rho^{\text{Au}} C_P^{\text{Au}} = 2.404 \cdot 10^6 \text{ J m}^{-3} \text{ K}^{-1}$ and $\rho^{\text{SiC}} C_P^{\text{SiC}} = 2.212 \cdot 10^6 \text{ J m}^{-3} \text{ K}^{-1}$.

and therefore

$$\tau_\ell^{-1} \sim \frac{1}{\rho C_P V} \frac{1}{4(k_0 d)} \int_0^\infty d\omega \frac{2\omega^3}{\pi^2 c^3} \text{Im}(\epsilon_S) \left. \frac{d\Theta(\omega, T)}{dT} \right|_{T_S} \times \left\{ \frac{1}{(k_0 d)^2} \frac{\text{Im}(\alpha^E)}{|\epsilon_S + 1|^2} + \text{Im}(\alpha^H) \left[\frac{1}{4} + \frac{1}{|\epsilon_S + 1|^2} \right] \right\}. \quad (18)$$

From the structure of the previous expression we see clearly that the main contributions to $1/\tau_\ell$ come from the particle's electric and magnetic resonances [which are located at $\epsilon_P \approx -2$ and $\epsilon_P \rightarrow \infty$ as can be seen in Eqs. (10)-(11)] and from the evanescent modes in the surface (at $\epsilon_S \approx -1$). In other words, the decrease in the TRT can be attributed to the enhanced radiative heat transfer due to the coupling of the particle's (induced) dipole moment to the evanescent modes of the surface [13, 44]. In addition, it is also seen from (18) that, depending on the strengths of the electric and magnetic polarizabilities, the lifetime can be proportional to d^3 or d . For metals we

typically observe the latter, as the induction of Foucault's currents gives rise to a big magnetic contribution to the heat transfer [21, 23, 29], whereas for polar materials like SiC the electric LDOS dominates the heat flux [13, 43], producing a $1/d^3$ behavior.

B. Cooling in the intermediate and far-field regimes

On the other hand, for distances $d \gtrsim \lambda_{\text{th},P}$ we can derive the appropriate expressions by using the stationary phase method (see appendix B). We then obtain

$$D^E(\omega, d) \approx \frac{\omega^2}{\pi^2 c^3} \left[\frac{1}{2} + \text{Im} \left(\frac{1 - \sqrt{\epsilon_S}}{1 + \sqrt{\epsilon_S}} \frac{e^{2ik_0 d}}{4k_0 d} \right) \right], \quad (19)$$

$$D^H(\omega, d) \approx \frac{\omega^2}{\pi^2 c^3} \left[\frac{1}{2} - \text{Im} \left(\frac{1 - \sqrt{\epsilon_S}}{1 + \sqrt{\epsilon_S}} \frac{e^{2ik_0 d}}{4k_0 d} \right) \right]. \quad (20)$$

We see that the presence of the substrate makes the electric and magnetic LDOS oscillate around one half of the free space value, given by $\omega^2/2\pi^2 c^3$. This behavior is analogous to the fermionic density oscillation close to a defect in a Fermi fluid or to the electric charge screening in a pool of ions [30]. From (19)-(20) we get a simplified expression expression for the TRT, namely

$$\tau_\ell^{-1} \approx \frac{1}{\rho C_P V} \int_0^\infty d\omega 2 \left(\frac{\omega^3}{\pi^2 c^3} \right) \left. \frac{d\Theta(\omega, T)}{dT} \right|_{T_S} \times \left\{ \text{Im}(\alpha^E) \left[\frac{1}{2} + \text{Im} \left(\frac{1 - \sqrt{\epsilon_S}}{1 + \sqrt{\epsilon_S}} \frac{e^{2ik_0 d}}{4k_0 d} \right) \right] + \text{Im}(\alpha^H) \left[\frac{1}{2} - \text{Im} \left(\frac{1 - \sqrt{\epsilon_S}}{1 + \sqrt{\epsilon_S}} \frac{e^{2ik_0 d}}{4k_0 d} \right) \right] \right\}. \quad (21)$$

In the case where we have narrow dipolar resonances we can write

$$\int_0^\infty d\omega \text{Im}(\alpha^{E,H}) f(\omega) \approx \sum_{i=1}^{N_{E,H}} f(\omega_i^{E,H}) \int_0^\infty d\omega \text{Im}(\alpha^{E,H}), \quad (22)$$

where $f(\omega)$ is a smooth and arbitrary function that varies slowly on the scale of the widths of the resonances of $\text{Im}(\alpha^{E,H})$. Here ω_i^E (ω_i^H) are the electric (magnetic) dipole resonances of the particle and N_E (N_H) is their total number, and therefore we can simplify τ_ℓ^{-1} even further,

$$\tau_\ell^{-1} \approx F(\omega^E, T_S) \left[\frac{1}{2} + \text{Im} \left(\frac{1 - \sqrt{\epsilon_S}}{1 + \sqrt{\epsilon_S}} \frac{e^{2ik_E d}}{4k_E d} \right) \right] \int_0^\infty d\omega \text{Im}(\alpha^E) + F(\omega^H, T_S) \left[\frac{1}{2} - \text{Im} \left(\frac{1 - \sqrt{\epsilon_S}}{1 + \sqrt{\epsilon_S}} \frac{e^{2ik_H d}}{4k_H d} \right) \right] \int_0^\infty d\omega \text{Im}(\alpha^H), \quad (23)$$

where

$$F(\omega, T_S) = \frac{1}{\rho C_P V} \left(\frac{2\omega^3}{\pi^2 c^3} \right) \left. \frac{d\Theta(\omega, T)}{dT} \right|_{T_S}, \quad (24)$$

$k_E = \omega^E/c$, $k_H = \omega^H/c$, and we assumed that only one resonance of each type (E and H) is present. Expression (23) then shows clearly the behavior of the TRT for large distances (and narrow resonances): it oscillates in a superposition of two periods while decaying as $1/d$. In particular, when one polarizability strongly dominates the other [say, $F(\omega^E, T_S) \gg F(\omega^H, T_S)$], we should see a clean “monochromatic” sinc-like oscillation of period $2\pi/k_E$. Since this is precisely the case for SiC, that is exactly what we observe in Figure 2b. That we don’t have a similar behavior for gold is explained by (i) the fact that for Au particles we have $\omega^E \gg \omega_{th}$ for $T_S \approx 300K$, meaning that the electric dipole gives no contribution to the heat flux (because $F(\omega^E, 300) \approx 0$), and (ii) the very large width of the magnetic resonance, which invalidates approximation (22) and in practice smears out the magnetic contribution to the TRT, resulting in the behavior seen in Figure 2a.

C. Temperature dependence

Finally, we study the temperature dependence of the TRT. In Fig. 3 we show some numerical results of the TRT over the temperature for $d = 10\mu m$ and $d = 100nm$, i.e., in the far-field and near-field regimes neglecting the temperature dependence of the material parameters [45]. First of all, one can observe that the TRT decreases with increasing temperatures T_S . Hence, the hotter the environment, the faster the particle cools down (reminding that, in the linear approximation, $T_P = T_S + \Delta T$ with $\Delta T \ll T_S$). Note that in the given temperature range of 50–500 K the TRT varies enormously. For Au (SiC) particles at $d = 10\mu m$ it can be as big as 4 hours (98 minutes) at $T_S = 50K$, dropping all the way down to around 5 seconds (266 milliseconds) at $T_S = 500K$. Even more interesting is what happens in the near-field regime ($d = 100nm$), where the TRT variation is not so impressive for gold (from about 240 milliseconds at $T_S = 50K$ to 58 milliseconds at $T_S = 500K$) but still very large for SiC (around 5 minutes at $T_S = 50K$ and 0.3 milliseconds at $T_S = 500K$). This difference at close distances is readily understood in terms of the coupling to the surface modes of the substrate. For SiC we have surface waves that lie in the frequency region close to the maximum of the thermal function $F(\omega, 300)$ defined in (24), and so the heat exchange is quite large at those temperatures. By decreasing T_S , however, we shift $F(\omega, T_S)$ toward lower frequencies and strongly suppress the participation of the surface modes in the heat transfer, leading to the huge increase in the TRT. By contrast, the surface modes for Au lie at much higher frequencies, which means that they don’t play any significant role in the heat flux in the considered range and therefore can’t affect much the TRT.

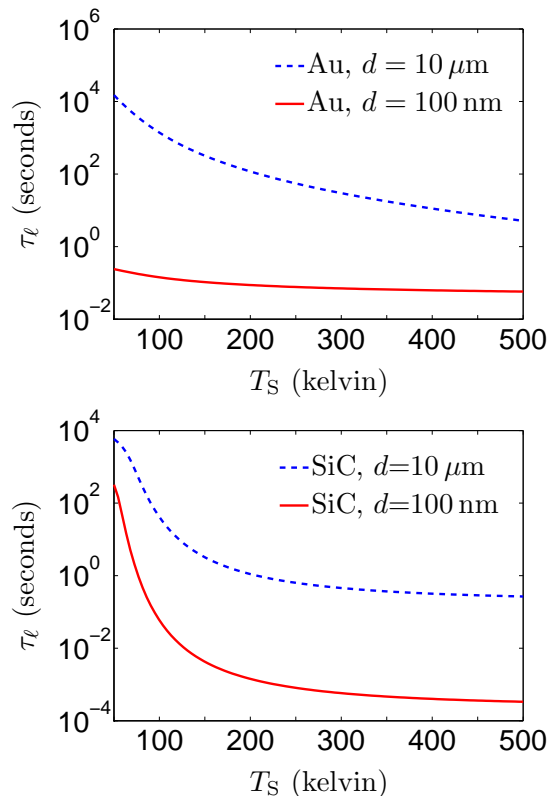


Figure 3: Semi-logarithmic plot of the temperature dependence of the TRT of a nanoparticle above a substrate at a fixed distance $d = 10\mu m$ and $d = 100nm$ for (a) a gold nanoparticle above a gold surface, (b) a SiC nanoparticle above a SiC surface. The particle radius is in both cases $R = 10nm$.

IV. DYNAMICS OF RELAXATION

The TRT defined in Eq. (14) is only useful for small temperature differences ΔT , since it is based on a linearization procedure. Here, we consider now the full dynamical process regarding the cooling of a particle by solving numerically the nonlinear Eq. (12). Here, we need to define the TRT in the general case: Let us assume that the nanoparticle is heated up with respect to its surrounding ($T_P > T_S$), then we define the thermal relaxation time of the particle as the elapsed time τ the particle needs to cool down to $T_S + \Delta T/e$. This definition ensures that for very small temperature differences we retrieve the linearized relaxation time τ_l defined in Eq. (14).

A. Cooling dynamics for an isolated particle

For an isolated particle we already saw that $D^E = D^H = D_0/2$, so that the cooling dynamics is governed by

the following equation

$$\frac{dT_P}{dt} = -\frac{1}{\rho C_p V} \sum_{i=E,H} \int_0^\infty d\omega \left(\frac{\omega^3}{\pi^2 c^3} \right) \text{Im}(\alpha^i) \Delta\Theta(\omega, T_P, T_S). \quad (25)$$

In Fig. 4 we show the results obtained by a numerical integration of Eq. (25) using a Runge-Kutta method with adaptive time steps. As for the initial conditions, we consider two different cases: (i) The solid lines show the TRT (as defined above) for $T_S = 300\text{K}$ and $T_P(t=0) = 300\text{K} + \Delta T$, while (ii) the dotted lines correspond to $T_S = 300\text{K} - \Delta T$ and $T_P(t=0) = 300\text{K}$. It can be seen in Fig. 4 that in the first case the TRT decreases with respect to ΔT , whereas in the second case it increases. This somewhat unexpected result shows that the cooling rate strongly depends not only on the temperature *difference* between particle and environment, but also on the *absolute* temperature of the environment. The first scenario can be qualitatively understood from the fact that by heating up the particle (while T_S is kept constant) the radiated power increases nonlinearly with T_P , leading therefore to a faster cooling. In the second case the radiative power of the particle at $t=0$ is kept constant while T_S is cooled down. Thus the increasing difference between T_P and T_S leads to an increase of the time the particle needs to cool down to $T_S + \Delta T/e$.

B. Cooling dynamics of a dipole near a surface

Now we look at the evolution of the temperature of a slightly heated nanoparticle near a surface. In Fig. 5 we show the time evolution of T_P for a gold nanoparticle with $R = 100\text{ nm}$ for a distance $d = 500\text{ nm}$ above a gold surface and a SiC nanoparticle above a SiC surface. As previously we consider a fixed particle temperature or a fixed surrounding temperature. As for the isolated particle, the exact relaxation times are in very good agreement with their linearized counterparts for $\Delta T \rightarrow 0$. We observe that due to the presence of the interface the TRT is much smaller than for the isolated particles. Apart from this we find the same qualitative behaviour as in the isolated case in Fig. 4.

V. CONCLUSIONS

We have investigated the thermal relaxation of a nanoparticle close to an interface. In particular, we have introduced a relaxation time τ_ℓ for the regime of small temperature differences between the particle and the surface and a generalized relaxation time τ for arbitrary temperature differences. Equipped with these definitions we have studied numerically the thermal relaxation of gold and SiC nanoparticles close to a gold or SiC surface, respectively. We have shown that the relaxation time behaves similarly to the lifetime of an atom close to

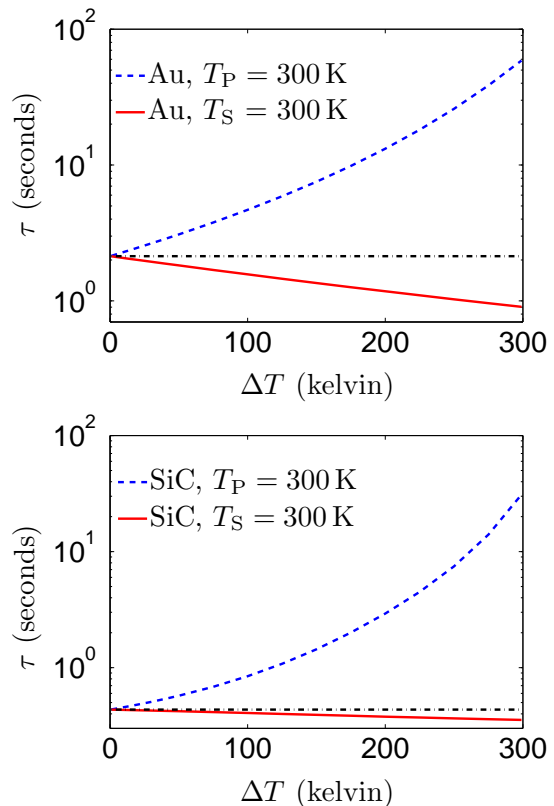


Figure 4: Semi-logarithmic plot of the TRT of a gold (a) and a SiC (b) nanoparticle with radius $R = 100\text{ nm}$ in free space, as a function of the temperature difference $\Delta T = T_P(0) - T_S$ (see text for further details). The horizontal line is the corresponding linearized TRT τ_ℓ .

a surface, varying rapidly for distances smaller than the thermal wavelength and finally dropping to zero. In addition, we found that the thermal relaxation time τ_ℓ is very sensitive to the temperature and can vary drastically - by several orders of magnitude - in the temperature range of $50 - 500\text{ K}$. We have identified all mechanisms which govern the thermal relaxation from subwavelength separation distances (in near-field regime) all the way to long separation distances (in far field regime).

This work can be generalized to the heating/cooling of a nano-object immersed in a more complex environment and exploited for the thermal management at nanoscale of complex plasmonic systems. Finally, a time-resolved scanning near-field optical microscopy as the one used in Refs. [46, 47] could be used to measure the time evolution of a substrate temperature in non-equilibrium situation by detecting, at the scale of TRT, the time variation of diffracted signal.

Acknowledgments

M. T. gratefully acknowledges support from the Stif- tung der Metallindustrie im Nord-Westen. P. B.-A. and

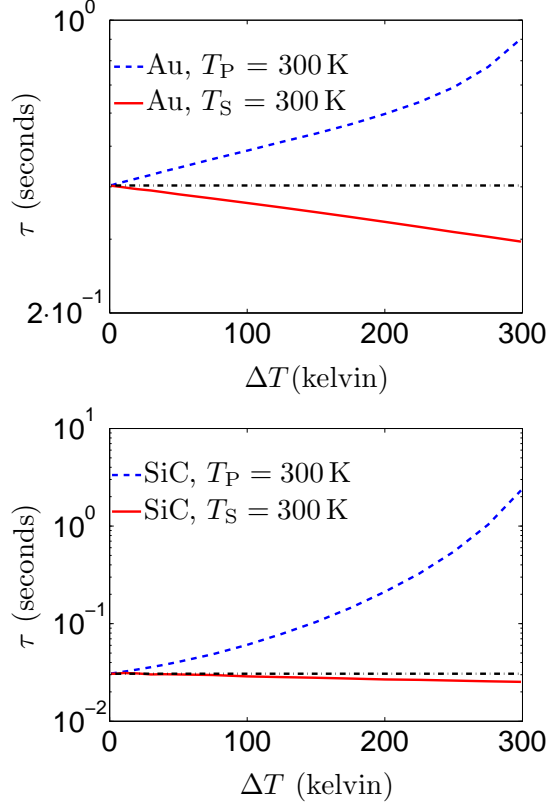


Figure 5: As in Fig. 4 but for a Au (SiC) particle above a Au (SiC) surface, at a distance of $d = 500$ nm.

F.S.S. R. acknowledges the support of the Agence Nationale de la Recherche through the Source-TPV project ANR 2010 BLANC 0928 01.

Appendix A: Green's dyadic for a flat interface

The Green's dyadic function with observation point $\mathbf{r} = (x, y, z)^t$ and source point $\mathbf{r}' = (x', y', z')^t$ above the flat surface, i.e., for $0 < z \leq z'$ can be expressed as [32, 33, 48]

$$\begin{aligned} \mathbf{G}^{(0)}(\mathbf{r}, \mathbf{r}'; \omega) = & \int \frac{d^2\kappa}{(2\pi)^2} \frac{ie^{i\kappa \cdot (\mathbf{x} - \mathbf{x}')}}{2\gamma_0} \\ & \times \left[\mathbb{1}_{--} e^{i\gamma_0(z' - z)} + \mathbb{R}_{+-} e^{i\gamma_0(z' + z)} \right] \\ & - \frac{1}{3k_0^2} \delta(z - z') \delta(\mathbf{x} - \mathbf{x}') \mathbf{e}_z \otimes \mathbf{e}_z \end{aligned} \quad (\text{A1})$$

where \mathbf{e}_z is the unit vector in z -direction and \otimes symbolizes the dyadic product. The tensors $\mathbb{1}$ and \mathbb{R} are defined

as

$$\mathbb{1}_{--} = \sum_{j=\{s,p\}} \hat{\mathbf{a}}_j^-(\boldsymbol{\kappa}) \otimes \hat{\mathbf{a}}_j^-(\boldsymbol{\kappa}) \quad (\text{A2})$$

$$\mathbb{R}_{+-} = \sum_{j=\{s,p\}} r_j \hat{\mathbf{a}}_j^+(\boldsymbol{\kappa}) \otimes \hat{\mathbf{a}}_j^-(\boldsymbol{\kappa}) \quad (\text{A3})$$

where

$$\hat{\mathbf{a}}_s^-(\boldsymbol{\kappa}) = \hat{\mathbf{a}}_s^+(\boldsymbol{\kappa}) = \frac{1}{\kappa} (-k_y, k_x, 0)^t, \quad (\text{A4})$$

$$\hat{\mathbf{a}}_p^-(\boldsymbol{\kappa}) = -\frac{1}{\kappa k_0} (k_x \gamma_0, k_y \gamma_0, \kappa^2)^t, \quad (\text{A5})$$

$$\hat{\mathbf{a}}_p^+(\boldsymbol{\kappa}) = \frac{1}{\kappa k_0} (k_x \gamma_0, k_y \gamma_0, -\kappa^2)^t \quad (\text{A6})$$

are the polarization vectors for s- and p-polarization. Note that these vectors are always orthogonal, but only have a unitary norm for propagating modes with $\kappa < k_0$. The reflection coefficients r_s and r_p are the usual Fresnel coefficients in Eqs. (6) and (7).

Appendix B: Density of states in the intermediate and far-field regimes

We describe here the asymptotic expansion of the TRT in the far-field regime. To this end we start from the expressions for the electric and magnetic LDOS from Eqs. (4) and (5) and take only the propagating modes into account. The distance independent part can be separated from the distance dependent part, so that the LDOS can be written as

$$D^E(\omega) = \frac{D_0}{2} + \text{Re} \int_0^{k_0} \frac{d^2\kappa}{(2\pi)^2} \frac{D_0}{4k_0\gamma_0} \left[r_s + \frac{2\kappa^2 - k_0^2}{k_0^2} r_p \right] e^{2i\gamma_0 d} \quad (\text{B1})$$

$$D^H(\omega) = \frac{D_0}{2} + \text{Re} \int_0^{k_0} \frac{d^2\kappa}{(2\pi)^2} \frac{D_0}{4k_0\gamma_0} \left[r_p + \frac{2\kappa^2 - k_0^2}{k_0^2} r_s \right] e^{2i\gamma_0 d} \quad (\text{B2})$$

where $D_0 = \omega^2/(\pi^2 c^3)$. That means for the distance dependent part we have two-dimensional integrals of the form ($i = E, H$)

$$I_i = \text{Re} \int d^2\kappa F_i(\kappa) e^{i\phi(\kappa)} \quad (\text{B3})$$

which have a highly oscillating integrand for $\phi(\kappa)$ larger than one, which corresponds in our case to distances larger than the wavelength. By using the stationary phase method [49] such integrals can be approximated by

$$I_i \approx \text{Re} \frac{2\pi}{i\sqrt{ac - b^2}} F_i(\kappa_s) e^{i\phi(\kappa_s)} \quad (\text{B4})$$

where κ_s is defined such that

$$\left. \frac{\partial \phi}{\partial k_x} \right|_{\kappa_s} = \left. \frac{\partial \phi}{\partial k_y} \right|_{\kappa_s} = 0 \quad (\text{B5})$$

and

$$a = \left. \frac{\partial^2 \phi}{\partial k_x^2} \right|_{\kappa_s}, \quad b = \left. \frac{\partial^2 \phi}{\partial k_x \partial k_y} \right|_{\kappa_s}, \quad \text{and} \quad c = \left. \frac{\partial^2 \phi}{\partial k_y^2} \right|_{\kappa_s}. \quad (\text{B6})$$

In our case $\phi(\kappa) = 2\gamma_0 d$ so that $\kappa_s = (0, 0)^t$ and $a = c = 2d/k_0$ and $b = 0$. Hence, by inserting these results into Eq. (B4) we find the far-field expressions in Eqs. (19) and (20).

Appendix C: Heat Capacity

In order to describe the heat capacity of the two considered materials (Au and SiC) we use a standard Debye

model [50]

$$C_V = 9n_a \frac{N_A k_B}{M} \left(\frac{T}{\Theta_D} \right) \int_0^{\Theta_D/T} dx \frac{x^4 e^x}{(e^x - 1)^2}, \quad (\text{C1})$$

where $N_A = 6.022 \cdot 10^{23} \text{ mol}^{-1}$ is Avogadro's constant, M is the molar mass and n_a the number of atoms or ions per unit cell, and Θ_D is Debye's temperature. For convenience we assume that $C_V \approx C_p$. When using the parameters $\Theta_D^{\text{Au}} = 170 \text{ K}$, $n_a^{\text{Au}} = 1$, $M^{\text{Au}} = 196.97 \text{ g mol}^{-1}$ and $\Theta_D^{\text{SiC}} = 1100 \text{ K}$, $n_a^{\text{SiC}} = 2$, $M^{\text{SiC}} = 40.1 \text{ g mol}^{-1}$ we get values for C_p which are in very good agreement with experimental and numerical results [51–54].

-
- [1] K. H. Drexhage, H. Kuhn, and F. P. Schäfer, Ber. Bunsenges. Phys. Chem. **72**, 1179 (1968).
 - [2] R. R. Chance, A. Prock, and R. Silbey, Adv. Chem. Phys. **37**, 1 (1978).
 - [3] P. W. Milonni, *The Quantum Vacuum*, (Academic Press, San Diego, 1994)
 - [4] L. Novotny and B. Hecht, *Principles of Nano-Optics*, (Cambridge University Press, Cambridge, 2006).
 - [5] G. W. Ford and W. H. Weber, Phys. Rep. **113**, 195 (1984).
 - [6] W. L. Barnes, J. Mod. Opt. **45**, 661 (1998).
 - [7] C. Henkel and V. Sandoghdar, Opt. Commun. **158**, 250 (1998).
 - [8] S. Basu, Z. M. Zhang, and C. J. Fu, Int. J. En. Res. **33**, 1203 (2009).
 - [9] V. P. Carey, G. Chen, C. Grigoropoulos, M. Kaviany, and A. Majumdar, Nanoscale Microscale Thermophys. Eng. **12**, 1 (2008).
 - [10] S. M. Rytov, Y. A. Kravtsov, and V. I. Tatarskii, Principles of Statistical Radiophysics (Springer, New York), Vol. 3. (1989).
 - [11] I. A. Dorofeyev, J. Phys. D: Appl. Phys. **31**, 600 (1998).
 - [12] J. B. Pendry, J. Phys.: Condens. Matter **11**, 6621 (1999).
 - [13] J.-P. Mulet, K. Joulain, R. Carminati, and J.-J. Greffet, Appl. Phys. Lett. **78**, 2931 (2001).
 - [14] A. I. Volokitin and B. N. J. Persson, Phys. Rev. B **65**, 115419 (2002).
 - [15] Yu. V. Martynenko and L. I. Ognev, Tech. Phys. **50**, 1522 (2005).
 - [16] G. V. Dedkov and A. A. Kyasov, Tech. Phys. Lett. **33**, 305 (2007).
 - [17] S.-A. Biehs, O. Huth, and F. Rüting, Phys. Rev. B **78**, 085414 (2008).
 - [18] F. Rüting, S.-A. Biehs, O. Huth, M. Holthaus, Phys. Rev. B **82**, 115443 (2010).
 - [19] A. Kittel, U. Wischnath, J. Welker, O. Huth, F. Rüting, and S.-A. Biehs, Appl. Phys. Lett. **93**, 193109 (2008).
 - [20] S.-A. Biehs and J.-J. Greffet, Phys. Rev. B **81**, 245414 (2010).
 - [21] O. Huth, F. Rüting, S.-A. Biehs, and M. Holthaus, Eur. Phys. J. Appl. Phys. **50**, 10603 (2010).
 - [22] S.-A. Biehs, O. Huth, F. Rüting and M. Holthaus, J. Appl. Phys. **108**, 014312 (2010).
 - [23] P.-O. Chapuis, M. Laroche, S. Volz, and J.-J. Greffet, Phys. Rev. B **77**, 125402 (2008).
 - [24] P. Ben-Abdallah, Appl. Phys. Lett. **89**, 113117 (2006).
 - [25] P. Ben-Abdallah, K. Joulain, J. Drevillon and C. Le Goff, Phys. Rev. B **77**, 075417 (2008).
 - [26] P. Ben-Abdallah, S.-A. Biehs, and K. Joulain, Phys. Rev. Lett. **107**, 114301 (2011).
 - [27] G. Domingues, S. Volz, K. Joulain, and J.-J. Greffet, Phys. Rev. Lett. **94**, 085901 (2005).
 - [28] A. Pérez-Madrid, J. M. Rubí, and L. C. Lapas, Phys. Rev. B **77**, 155417 (2008).
 - [29] P.M. Tomchuk, N.I. Grigorchuk, Phys. Rev. B **73**, 155423 (2006).
 - [30] K. Joulain, R. Carminati, J.-P. Mulet, and J.-J. Greffet, Phys. Rev. B **68**, 245405 (2003).
 - [31] A. Narayanaswamy and G. Chen, J. Quant. Spectrosc. Radiat. Transf. **111**, 1877 (2010).
 - [32] Chen-To Tai (1971), *Dyadic Green's Functions in Electromagnetic Theory*, Intext Educational Publishers, Scranton.
 - [33] K. Joulain, J.-P. Mulet, F. Marquier, R. Carminati, and J.-J. Greffet, Surface Science Reports **57** 59 (2005).
 - [34] J. D. Jackson, *Classical Electrodynamics*, 3rd ed., (John Wiley, New York, 1998).
 - [35] C. F. Bohren and D. R. Huffman, *Absorption and Scattering of Light by Small Particles* (Wiley Science, New York, 1998).
 - [36] G. W. Kattawar and M. Eisner, Appl. Opt. **9**, 2685 (1970).
 - [37] C. Henkel and K. Joulain, Appl. Phys. B: Lasers and Optics **84** 61-68 (2006).
 - [38] I. Dorofeyev, Physics Letters A **363**, 251 (2007).
 - [39] P.-O. Chapuis, S. Volz, C. Henkel, K. Joulain, and J.-J. Greffet, Phys. Rev. B **77**, 035431 (2008).
 - [40] H. R. Haakh and C. Henkel, Eur. Phys. J. B (2011) (submitted).
 - [41] R. Rupp, Phys. Rev. B **11**, 2871 (1975).
 - [42] R. Rupp, Phys. Rev. B **45**, 11209 (1992).
 - [43] A. V. Shchegrov, K. Joulain, R. Carminati, and J.-J. Greffet, Phys. Rev. Lett. **85**, 1548 (2000).
 - [44] Y. Chalopin, H. Dammak, M. Laroche, M. Hayoun, and J.-J. Greffet, Phys. Rev. B **84**, 224301 (2011).

- [45] I. Dorofeyev, Phys. Lett. A **372**, 1341 (2008).
- [46] E. Rousseau, A. Siria, G. Jourdan, S. Volz, F. Comin, J. Chevrier, and J.-J. Greffet, Nature Photonics **3**, 514 (2009).
- [47] P. van Zwol, L. Ranno, and J. Chevrier, arXiv:1111.1193v1 (2011).
- [48] J. E. Sipe, J. Opt. Soc. Am. B **4**, 481 (1987).
- [49] S. K. Cho, *Electromagnetic Scattering*, (Springer, New York, 1990).
- [50] N. Ashcroft and N. D. Mermin, *Solid-State Physics*, (Saunders, Philadelphia, 1976).
- [51] T. H. Geballe and W. F. Giauque, J. Am. Chem. Soc. **74**, 2368 (1952).
- [52] K. Karch, P. Pavone, W. Windl, O. Schütt, and D. Strauch, Phys. Rev. B **50**, 17054 (1994).
- [53] A. Zywietz, K. Karch, and F. Bechstedt, Phys. Rev. B **54**, 1791 (1996).
- [54] L. J. Porter, J. Li, and S. Yip, J. Nucl. Mat. **246**, 53 (1997).